SAND2015-4636C

9^{th} U. S. National Combustion Meeting
Organized by the Central States Section of the Combustion Institute
May 17-20, 2015
Cincinnati, Ohio

Time-resolved measurements of product formation in neopentane oxidation: a probe to investigate chain-branching mechanism

A. J. Eskola, I. O. Antonov, L. Sheps, J. D. Savee, D. L. Osborn, C. A. Taatjes

Combustion Research Facility, Sandia National Laboratories, 7011 East Avenue, MS 9055, Livermore, California 94551, USA
Corresponding author: ajeskol@sandia.gov

Abstract: Ketohydroperoxide formation and decomposition was investigated in time-resolved, Cl-atom initiated neopentane oxidation experiments in the temperature range 550 K – 725 K using a photoionization time-of-flight mass spectrometer. Ionization light was provided either by the Advanced Light Source tunable synchrotron radiation or ~ 10.2 eV fixed energy radiation from a H_2-discharge lamp. Experiments were performed both at 1 – 2 atm pressure using a high-pressure reactor and also at ~ 9 Torr pressure employing a low-pressure reactor for comparison. Due to the highly symmetric structure of neopentane, ketohydroperoxide signal is concluded to originate from a 3-hydroperoxy-2,2-dimethylpropanal isomer, *i.e.* from a γ-ketohydroperoxide (γ-KHP). Also, the photoionization spectra of the γ-KHP measured at low- and high pressures and varying oxygen concentrations agree well with each other, further supporting they originate from the single isomer. In addition to detection of ketohydroperoxide for the first time in neopentane oxidation experiments, measurements performed in this work both at low and high pressures also strongly suggest that Korcek mechanism play potentially an important role in the decomposition of γ-KHP observed.

Keywords: Neopentane, Autoignition, Ketohydroperoxide, Chain-Branching

1. Introduction

Low-temperature oxidation plays a critical role in the autoignition of fuel-air mixture, understanding of which is crucial in the development of new low emission, high efficiency engine technologies.[1, 2] Low-temperature oxidation of a saturated hydrocarbon is initiated by formation of alkyl radical R that further reacts with O_2. The R + O_2 reaction proceeds via formation of alkyl peroxy radical, RO_2, which can subsequently decompose back to reactants or isomerize:

$$R + O_2 \leftrightarrow RO_2 \rightarrow \qquad (1)$$

In addition, for an alkyl radical that has hydrogen(s) in β-position with respect to the radical site, both direct elimination from chemically excited RO_2 and thermal decomposition of RO_2 lead to formation of alkene + HO_2 products.

$$RO_2 \rightarrow HO_2 + \text{alkene} \qquad (2)$$

However, the radical of interest in this work, neopentyl radical $(CH_3)_3CCH_2$, formed in Cl-atom + neopentane reaction, does not have any β-hydrogen and thus reaction channel (2) is absent. This property makes neopentane an excellent radical source to investigate the chain-branching mechanism experimentally under low-temperature oxidation conditions where hydroperoxyalkyl radical QOOH plays a crucial role. The most efficient formation of QOOH radical is when RO_2 isomerizes to QOOH *via* six-member transition state.

$$RO_2 \leftrightarrow QOOH \qquad (3)$$

Carbon-centered QOOH radicals can dissociate to O-heterocycle (cyclic ether) and OH-radical in a chain-propagation reaction

$$QOOH \rightarrow \text{O-heterocycle} + OH \qquad (4)$$

or, in competition with reaction (4), react again with O_2, especially at high pressures ($p \geq 1$ atm) when $[O_2]$ is also high. Reaction (5) is essential for autoignition because it initiates a mechanism that leads to chain-branching.

$$QOOH + O_2 \leftrightarrow OOQOOH \qquad (5)$$

The hydroperoxyalkylperoxy radical OOQOOH can efficiently isomerize to HOOQ`OOH radical which immediately decomposes to OH + HOOQ`O, the latter of which is called ketohydroperoxide (KHP) since it contains both ketone or aldehyde functionality and a hydroperoxy group.

$$OOQOOH \leftrightarrow HOOQ`OOH \rightarrow OH + HOOQ`O\ (KHP) \qquad (6)$$

Ketohydroperoxide HOOQ`O is a labile closed-shell molecule that can further thermally decompose and release the second OH radical, effectively leading to chain-branching, *i.e.* together reactions (6) and (7) produce two OH radicals and an OQ`O radical.

$$HOOQ`O \rightarrow OH + OQ`O \qquad (7)$$

The oxygen-centered OQ`O radical can also lead to reactive radicals and thus increase system reactivity even more.

Low-temperature oxidation of neopentane has received much attention before, probably due to its simple molecular structure, where all hydrogens are primary and identical. Walker et al. added neopentane to slowly reacting mixtures of H_2/O_2 at 753 K and determined primary and secondary products under low-temperature oxidation conditions.[3, 4] Curran et al.[5] constructed a detailed chemical kinetic model on neopentane oxidation and simulated experimental results of Walker et al.[3, 4]. Of interest to the current work, their model underpredicted methylpropanal formation and they suggested that there are probably other pathways leading to its formation. In a combined experimental and modelling flow reactor study of neopentane oxidation at 8 atmospheres, Wang and Curran et al.[6] both improved their model to fit experimental results and observed a significant formation of formic acid which their model, however, was not able to predict. Also interesting for the current work, significant [HCOOH] was observed already at lowest experimental temperatures, 620 K, where no other reaction products were noticed, and highest formic acid concentrations were measured around 650 K. Neopentane oxidation has also been studied in a temperature range 800 – 1230 K at 1, 5, and 10 atm pressures using the jet-stirred reactor (JSR) by Dagaut et al.[7], who also constructed a model to simulate their high-temperature experiments. Sun and Bozzelli[8] performed *ab initio* calculations at the CBS-Q level and master equation analysis to evaluate reaction paths and kinetics for neopentyl oxidation. DeSain et al.[9] measured time-resolved production of OH and HO_2 radicals in the pulsed-photolytic Cl-atom initiated oxidation of neopentane in the temperature range 573 – 750 K and at total pressures about 55 Torr. They also simulated their low-pressure results using a small ad hoc kinetic model. Interestingly, they observed a significant (about 3 ×) increase in HO_2 production intensity at 673 K once $[O_2]$ was increased from 7 to 60×10^{17} cm^{-3}. Although their model was not able to describe the observation, they suggested that it originated from chain-branching. Finally Petway et al.[10] extended measurements of DeSain et al. with some success as well as modelled their results using Reaction Mechanism Generator developed at MIT.

Although all neopentane oxidation models discussed above include chain-branching mechanism where KHP formation and decomposition plays a crucial role, ketohydroperoxide has not been observed experimentally before in any neopentane oxidation experiments. KHP formation was observed for the first time fairly recently in JSR low-temperature *n*-butane oxidation experiments[11] and first time-resolved KHP formation and decomposition experiments were published only very recently[12]. KHP formation is observed in the current neopentane oxidation experiments; particular attention is paid to understanding the KHP decomposition mechanism, which might also proceed *via* other mechanism(s) than shown above in equation (7).

2. Experimental

In this study both low-pressure ($p \sim 9$ Torr) and high-pressure ($p \sim 1 - 2$ atm) flow reactors were employed. The low-pressure reactor has been described in detail before [13] and the high-pressure reactor (HPR) has been presented recently[12]. Radical chemistry in the low- and high-pressure reactors was initiated by photolytic production of Cl-atoms which then reacted with neopentane producing neopentyl radicals in the presence of O_2. In both the low- and high-pressure reactor 248 nm photolysis of oxalyl chloride ($(ClCO)_2 \rightarrow 2\ Cl + 2\ CO$) was used to produce Cl-atoms; in the low-pressure reactor 351 nm photolysis of Cl_2 ($Cl_2 \rightarrow 2\ Cl$) and in the high-pressure reactor 193 nm photolysis of $CFCl_3$ ($CFCl_3 \rightarrow CFCl_2 + Cl$) were also employed. An uncoated tubular, heatable quartz reactor was used in low-pressure experiments. Most measurements with the HPR were performed using a metal reactor in contact with the reacting mixture, but several experiments were carried out using a more inert quartz tube in contact with photolytically initiated reacting mixture. The low-pressure reactor is sampled *via* a ~ 650 μm hole on the tube wall (*i.e.* orthogonal to the photolysis laser axis) whereas the HPR is sampled through a ~ 100 – 150 μm hole in the end-plate of the reactor (*i.e.* on the photolysis laser axis). The sampled molecular beam from the reactors was then skimmed and intersected by ionizing vacuum ultraviolet (VUV) tunable radiation from the Advanced Light Source (ALS) synchrotron. Some experiments were also performed using ~10.2 eV radiation from a H_2-discharge lamp. Ionized species were mass-separated using an orthogonal-acceleration, multiplexed photoionization time-of-flight mass spectrometer (MPIMS) where full mass spectra were taken at 20 μs intervals. In order to obtain more information on reaction isomers and product branching ratios, photoionization spectra were measured by scanning the energy of the ionizing synchrotron radiation.[14]

3. Results and Discussion

Scheme 1 shows a reaction mechanism for neopentane low-temperature oxidation starting from neopentyl radical and extending up to the KHP formation.[6] Experiments in the current work were performed both at low and high pressure. While kinetics of specific reactions in scheme 1 can change with pressure and thus effect on product yields, the overall oxidation mechanism should not change, meaning that scheme 1 is applicable to both low- and high-pressure results.

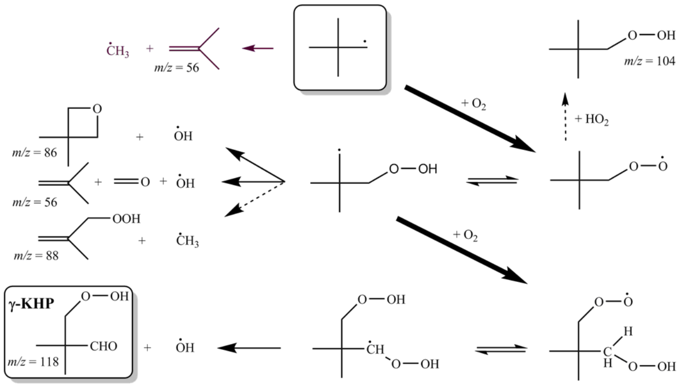

Scheme 1: Neopentane low-temperature oxidation reaction mechanism starting from neopentyl radical and extending up to γ-KHP formation.[6]

Figure 1 shows the time dependence of RO_2 and characteristic neopentane oxidation products which were measured at several temperatures using the low-pressure reactor. Neopentylperoxy radical RO_2 was observed at the radical R = C_5H_{11} nominal mass $m/z = 71$ (see fig.1a**)**, where also contribution from C_4H_7O signal can be noticed (see fig.1e), which is most likely a daughter ion of the KHP. Once the C_4H_7O signal contribution is subtracted, it becomes clear that only at highest temperature, 725 K, is all RO_2 consumed within the experimental time range, 40 ms. Fig. 1b shows signals observed at $m/z = 56$, which originate both from *i*-butene and from strong daughter ion of 3,3-dimethyloxetane at mass 56. Parent ion of 3,3-dimethyloxetane is extremely weak. In fig. 1c are shown signals observed at $m/z = 118$, which originate from the ketohydroperoxide, a γ-KHP where one –CH_2– group separates carbons containing an aldehyde and a hydroperoxy group. Clearly γ-KHP formation becomes stronger with increasing temperature. In these measurements $[O_2]$ was 5×10^{16} cm^{-3} and total density was kept constant. Finally fig. 1d shows $m/z = 72$ signals, originating mainly from methyl propanal, whose intensity increase strongly from 575 to 675 K, less so from 675 to 700, until at 725 K signal intensity is below that of 700 K. This change might be related to the γ-KHP decomposition, an important topic of this work and which we will discuss next.

Scheme 2 shows two mechanisms for the decomposition of γ-KHP (3-hydroperoxy-2,2-dimethylpropanal). Decomposition of γ-KHP *via* -O–OH bond rupture to two radicals, OH and oxy-radical (left), is the well-known KHP decomposition mechanism leading to chain-branching and is included in any kinetic model of hydrocarbon low-temperature oxidation. On the other hand, decomposition mechanism of γ-KHP through a cyclic peroxide intermediate to carbonyl compound and organic acid (right), known as Korcek decomposition, has been suggested theoretically[15] only very recently and its importance in gas phase chemistry is still very uncertain and definitely needs experimental work to be quantify its importance. Note that the Korcek decomposition is a chain-termination reaction mechanism, because it leads to two unreactive, closed shell species, thus it strongly *reduces* system reactivity. This is totally opposite to the decomposition *via* -O–OH bond rupture, which strongly *accelerates* system reactivity. Figure 2 shows that the main Korcek decomposition products of γ-KHP, formic acid and methylpropanal, are observed at low pressures in this work and their time-behavior is the same within experimental uncertainty, which suggest they originate from a same source, e.g. from Korcek decomposition. However, the ratio formic acid / methylpropanal = 0.33, differs from unity, indicating there must also be other source(s) of methylpropanal at low pressures.

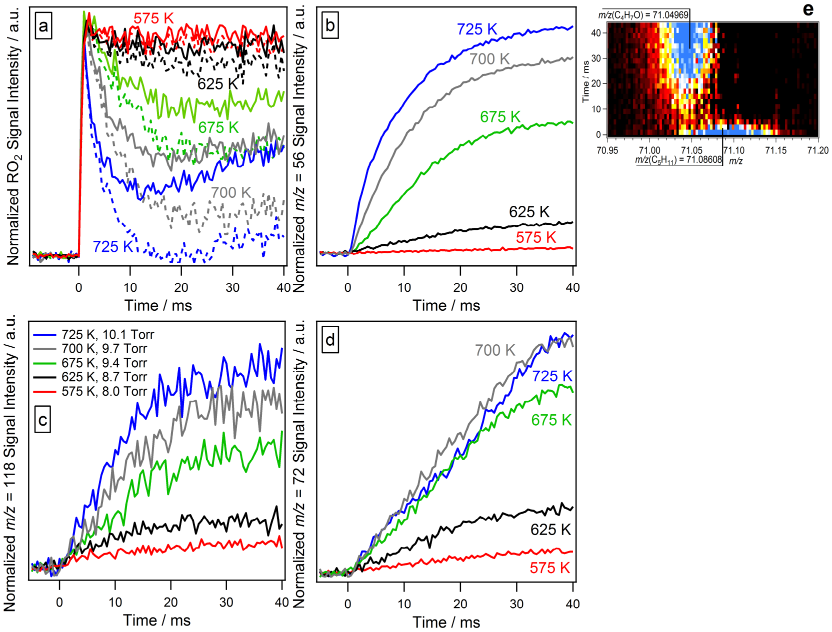

Figure 1: Time traces of product formation from Cl-atom initiated neopentane oxidation experiments performed at different temperatures using the low-pressure reactor ($[O_2] = 5 \times 10^{16}$ cm^{-3}, total density kept constant). **a**) Neopentylperoxy radical RO_2 observed at $m/z = 71$ (full line). Contribution from γ-KHP daughter subtracted (broken line, see **e**). **b**) Signal at $m/z = 56$ originates from *i*-butene and 3,3-dimethyloxetane. **c**) Signal at $m/z = 118$ comes from γ-KHP. **d**) Signal at $m/z = 72$ originates mainly from methylpropanal. **e**) 2-D time versus m/z -plot around nominal $m/z(RO_2) = 71$ from 700 K experiment shown in figure 1a. Significant product formation on $m/z(C_4H_7O) = 71.04969$ at later times, likely a γ-KHP daughter ion, in addition to rapid decay of C_5H_{11} signal ($m/z(C_5H_{11}) = 71.08608$) that originates from RO_2.

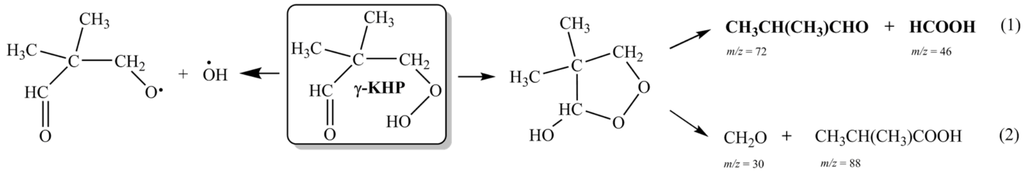

Scheme 2. γ-KHP decomposition *via* -O–OH bond rupture to two radicals (left) or through cyclic peroxide intermediate to carbonyl compound and organic acid (right), known as Korcek decomposition mechanism[15].

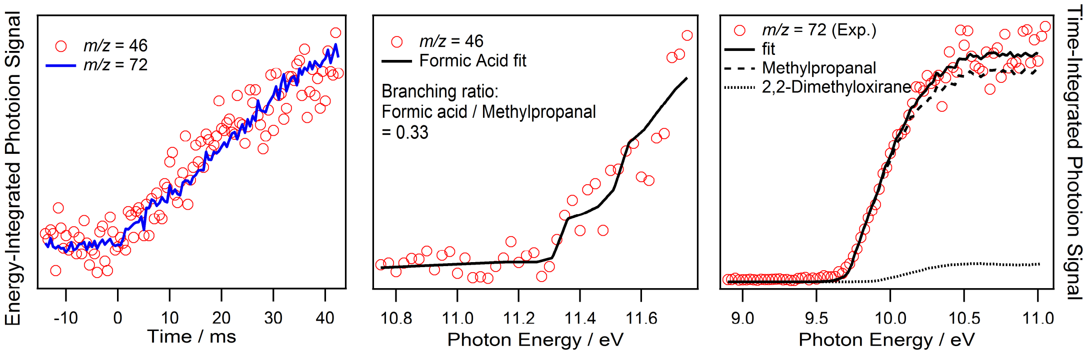

Figure 2. Suggested decomposition of γ-KHP at 8.7 Torr and 625 K to carbonyl (methyl propanal, *m/z* = 72) and organic acid (formic acid, *m/z* = 46) according to the Korcek decomposition mechanism through a cyclic peroxide intermediate. Time-behavior of *m/z* = 46 and 72 agree and PIE spectra of *m/z* = 46 and 72 signals originate from formic acid and methyl propanal, respectively.

Figure 3a shows kinetic time-traces of the γ-KHP formation in neopentane oxidation experiments at low- and high pressures. It can be seen that simultaneous increase in total pressure (× 100) and $[O_2]$ (× 50) at 625 K has only small effect on time profile. This effect was more pronounced in case of *n*-butane oxidation.[12] Figure 3b shows photoionization spectra from these same measurements, where experimental conditions were changed over wide ranges, yet no differences between spectra can be seen, strongly suggesting they originate from the same γ-KHP species, that is 3-hydroperoxy-2,2-dimethylpropanal (see scheme 1 and 2).

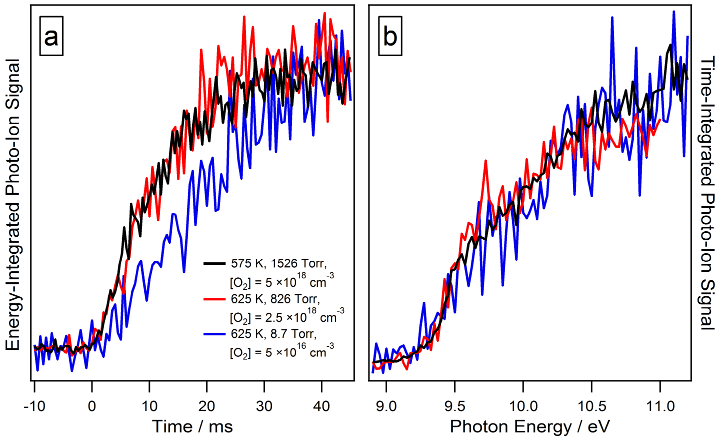

Figure 3. Kinetics (**a**) and photoionization spectra (**b**) of the γ-KHP observed in low- and high-pressure neopentane oxidation experiments performed in the current work.

Measurements at high pressures (*i.e.* $p \geq 1$ atm) are necessary to understand the effect of γ-KHP formation and decomposition kinetics on autoignition chemistry. Figure 4 shows results from Cl-atom initiated neopentane oxidation experiments which were performed using HPR at 1 atm pressure. It can be seen from figure 4a that signal intensities at *m/z* = 56 (isobutene and 3,3-dimethyloxetane), 72 (methylpropanal and 2,2-dimethyloxirane), and 118 (KHP) increase rapidly and in similar fashion with temperature from 550 to 650 K, after which signal intensities at *m/z* = 56 and 72 increase even faster with temperature, whereas γ-KHP signal at *m/z* = 118 stays constant. When temperature is still increased up to 700 K, spontaneous reaction was observed, *i.e.* very significant neopentane oxidation occurred without laser initiation. Note that the very stable $CFCl_3$ photolytic precursor was used. A possible explanation is that around 650 K γ-KHP starts to decompose, initiating chain reaction $\gamma\text{-KHP} \rightarrow X{*}OH \rightarrow X{*}OH + \text{neopentane} + O_2 \rightarrow X{*}C_5H_{11}OO \rightarrow X{*}QOOH + O_2 \rightarrow X{*}\gamma\text{-KHP}$ etc., where $X > 1$. However, at 650 K γ-KHP decomposition is still slow and has to compete with diffusion-limited losses on HPR walls. Product formation increases significantly once temperature is increased from 650 to 675 K, possibly due to the increased γ-KHP decomposition rate. Inset, fig. 4b, shows normalized RO_2 and γ-KHP signal time traces from 590 and 675 experiments. At 590 K, RO_2 signal clearly decays after nearly instantaneous formation following the photolysis, and γ-KHP formation is fairly slow, its intensity weak, and around 15 ms its concentration starts to decrease. However, upon increasing temperature up to 675 K, there are no signs of RO_2 decay but instead the signal continues to increase slowly after its almost instantaneous formation. The γ-KHP formation is much faster than at 590 K and, interestingly, γ-KHP signal increases up to 30 ms after the photolysis. This continuous increase in γ-KHP signal at higher temperature probably originates from increasingly fast chain-reaction discussed above. At only a little higher temperature oxidation was spontaneous.

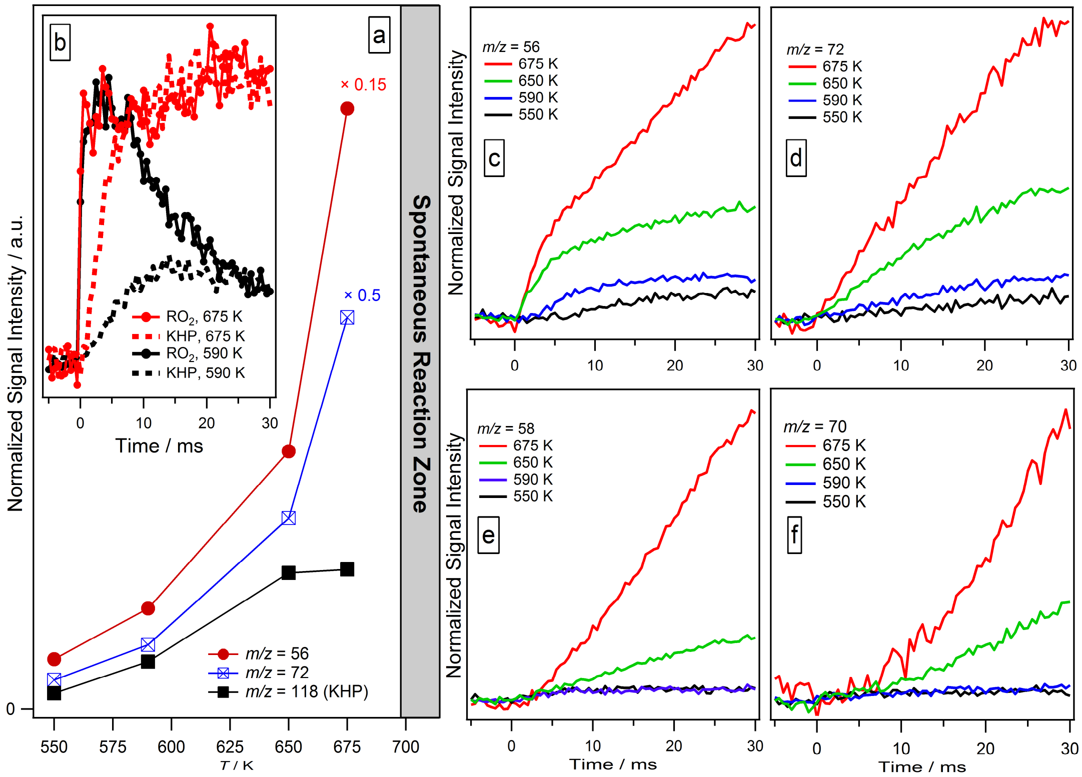

Figure 4. Results from Cl-atom initiated neopentane oxidation experiments performed at about 1 atm pressure using the HPR without quartz tube and keeping total density constant and $[O_2] = 2.5 \times 10^{18}$ cm^{-3} (H_2-discharge lamp employed). **a**) Normalized signal intensities at *m/z* = 56, 72, and 118 *versus* temperature. At 700 K and higher temperatures spontaneous reaction occurred in the HPR. Inset (**b**) shows normalized RO_2 and γ-KHP signal time traces at 590 K and 675 K. (**c - f**) Normalized product signal time traces at *m/z* = 56, 72, 58, and 70.

Figures 4c – 4f show normalized product signal time traces at *m/z* = 56, 72, 58, and 70 from the same experiments as shown in figures 4a and 4b. It is fairly obvious that *m/z* = 56 signal in figure

4c has two components, a rapid formation starting at time zero followed by a slower formation which becomes significantly faster as temperature is increased. This is in agreement with mechanism of scheme 1 where rapid component originates from thermal decomposition of almost instantaneously formed RO_2 whereas slower formation that can be observed at higher temperatures, largely originates from chain-reactions initiated by γ-KHP decomposition. Importantly, signals at *m/z* = 72 do not show any rapid component of formation nor is there any product at this mass in scheme 1. Instead, time-behavior of *m/z* = 72 suggest it is a secondary oxidation product, which agree with its formation as a product of γ-KHP decomposition *via* Korcek decomposition mechanism shown in scheme 2. Another product of Korcek reaction channel (1), formic acid (IE = 11.33 eV), was not observed in these experiments because energy of H_2-discharge lamp (~ 10.2 eV) employed was not high enough to ionize HCOOH. In Cl-atom initiated neopentane oxidation experiments performed at the ALS using synchrotron radiation at 1526 Torr and 575 K conditions (see figure 5), formation of formic acid (*m/z* = 46) and methylpropanal (*m/z* = 72) were observed to have the same time-behavior, which is very similar to that observed in figure 4d. In addition, at 1526 Torr and 575 K conditions, a branching ratio formic acid / methyl propanal = 1.17 was determined by fitting absolute photo-ionization cross-sections to the experimental photoionization spectra as shown in figure 5. The value obtained, 1.17, is close to unity, suggesting that in these time-resolved experiments γ-KHP decomposition *via* Korcek mechanism indeed occurred.

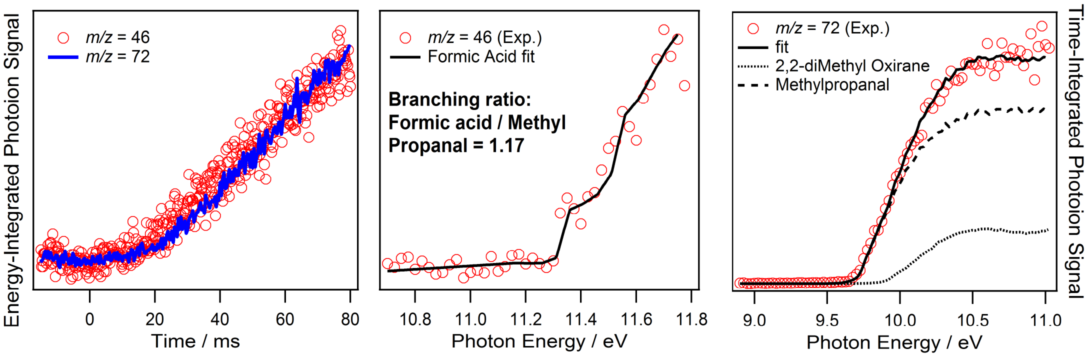

Figure 5. Decomposition of γ-KHP at 1526 Torr, 575 K to carbonyl (methyl propanal, *m/z* = 72) and organic acid (formic acid, *m/z* = 46) according to the Korcek. Time-behavior of *m/z* = 46 and 72 agree and PIE spectra of *m/z* = 46 and 72 signals originate from formic acid and methyl propanal, respectively.

Figures 4e and 4f show signals at *m/z* = 58 and 70. There are certain characteristics that these two signals share and, on the other hand, separate them from signals shown in figures 4a – 4d. First, there is essentially no change in very small signal intensities at *m/z* = 58 and 70 once temperature is increased from 550 K to 590 K whereas at *m/z* = 56, 72, and 118 there is a clear increase in signal intensities. On the other hand, signal intensities at *m/z* = 58 and 70 increase notably when temperature is increased to 650 K, but this increase is especially dramatic once temperature is increased from 650 K to 675 K, only 25 K. No similar behavior is seen at *m/z* = 56, 72, and 118. In addition, signals time behavior at *m/z* = 58 and 70 seem to lag behind signals behavior at *m/z* = 72. These observations are in agreement with the mechanism shown in scheme 3, where *m/z* = 58 and 70 signals originate from isobutanal-2-methyloxy radical reaction with O_2 to form acetone (*m/z* = 58) and methacrolein (*m/z* = 70). Here isobutanal-2-methyloxy radical is formed in γ-KHP decomposition *via* -O–OH bond scission. This conclusion is in agreement with observations of Wang and Curran et al.[6] who observed significant formic acid formation, characteristic sign of Korcek reaction, but no acetone or methacrolein at 625 K in their neopentane oxidation experiments at 8 atm. However, already at 690 K their acetone mole fraction was ~ 5 times higher than formic acid mole fraction and methacrolein mole fraction was close to that of formic acid.

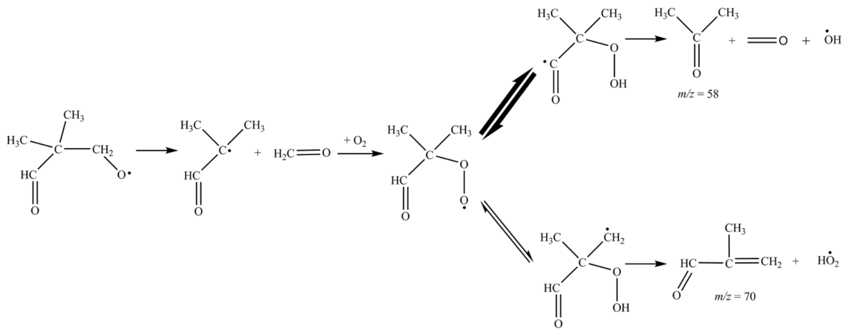

Scheme 3: Main pathways from isobutanal-2-methyloxy radical, formed in decomposition of γ-KHP to $HCOC(CH_3)_2CH_2O$ + OH, in neopentane low-temperature oxidation experiments.[6]

In addition to the current direct, time-resolved observation of formic acid and methyl propanal formation with similar yield in high pressure neopentane oxidation experiments, presumably from the Korcek decomposition of γ-KHP, results from a few previous measurements also suggest the presence of this reaction. As was already notice in the introduction section, in the detailed modelling work of Walker et al.[3, 4] experimental results, Curran et al.[5] observed more methyl propanal formation than their model was able to predict; we can now suggest that additional portion of methyl propanal originated from the Korcek decomposition of γ-KHP. The Korcek decomposition was not included in the Curran et al.[5] model. Similarly, in a combined experimental and modelling flow reactor study of neopentane oxidation, Wang and Curran et al.[6] observed a significant formation of formic acid which their model, however, was not able to predict. Note that their model did not include Korcek decomposition mechanism nor was methyl propanal measured in their experimental setup. Also interesting for the current work, Wang and Curran et al.[6] observed significant [HCOOH] formation already at lowest experimental temperatures, 620 K, where no other reaction products were noticed. Wang and Curran et al. observations above are in agreement with the Korcek decomposition of γ-KHP to form formic acid and methyl propanal through a reaction channel with lowest rate-limiting energy barrier, which is effective already at temperatures where γ-KHP decomposition via -O–OH bond rupture is negligible. This, on the other hand, is in agreement with theoretical results of Jalan et al.[15]. Finally, competition between the two γ-KHP decomposition mechanisms, *i.e.* between the classical -O–OH bond rupture to two radicals or the Korcek decomposition to carbonyl compound and organic acid, might explain results of fig. 1d where intensities of *m/z* = 72 signal, originating mainly from methyl propanal, increase strongly from 575 to 675 K, less from 675 to 700, until at 725 K signal intensity is below that of 700 K. It is possible that at lower temperatures the Korcek decomposition of γ-KHP, which proceeds over a tight transition state, leads to the observed stronger methyl propanal formation as temperature is increased until at higher temperatures around 700 K the classical -O–OH bond rupture mechanism, which is about 15 kcal more endothermic than Korcek mechanism but proceeds over a loose transition state, finally win. This then results to decreasing signal intensity at *m/z* = 72.

4. Conclusions

In this work KHP formation in neopentane low-temperature oxidation conditions was observed experimentally for the first time. In addition, products and yields of Korcek decomposition of γ-KHP were observed and quantified, suggesting that this very recent theoretically predicted mechanism play a role in gas-phase neopentane oxidation. Although the major neopentane Korcek decomposition products, formic acid and methyl propanal, have been observed previously, in this work these products are observed simultaneously in time-resolved manner, providing new experimental support for this mechanism.

5. Acknowledgements

This material is based upon work supported by the U.S. Department of Energy, Office of Science, Office of Basic Energy Sciences (DOE/BES). I.O.A and L.S. are supported by DOE/BES under the Argonne-Sandia Consortium on High-Pressure Combustion Chemistry. Sandia is a multiprogram laboratory operated by Sandia Corporation, a Lockheed Martin Company, for the United States Department of Energy's National Nuclear Security Administration under contract DEAC04-94AL85000. This work used resources of Advanced Light Source, an Office of Science User Facility supported by the Director, Office of Science, Office of Basic Energy Sciences, of the U.S. Department of Energy under Contract No. DE-AC02-05CH11231.

6. References

1. C. K. Westbrook, Proc. Combust. Inst. 28 (2000) 1563-1577
2. J. E. Dec, Proc. Combust. Inst. 32 (2009) 2727-2742 doi:10.1016/j.proci.2008.08.008.
3. R. R. Baker; R. R. Baldwin; C. J. Everett; R. W. Walker, Combust. Flame 25 (1975) 285-300
4. R. R. Baker; R. R. Baldwin; R. W. Walker, Combust. Flame 27 (1976) 147-161
5. H. J. Curran; W. J. Pitz; C. K. Westbrook; M. W. M. Hisham; R. W. Walker, Proc. Combust. Inst. 26 (1996) 641-649
6. S. Wang; D. L. Miller; N. P. Cernansky; H. J. Curran; W. J. Pitz; C. K. Westbrook, Combust. Flame 118 (1999) 415-430
7. P. Dagaut; M. Cathonnet, Combust. Flame 118 (1-2) (1999) 191-203 10.1016/s0010-2180(98)00147-3.
8. H. Sun; J. W. Bozzelli, J. Phys. Chem. A 108 (10) (2004) 1694-1711
9. J. D. DeSain; S. J. Klippenstein; C. A. Taatjes, Phys. Chem. Chem. Phys. 5 (2003) 1584-1592
10. S. V. Petway; H. Ismail; W. H. Green; E. G. Estupiñán; L. E. Jusinski; C. A. Taatjes, J. Phys. Chem. A 111 (2007) 3891-3900
11. F. Battin-Leclerc; O. Herbinet; P.-A. Glaude; R. Fournet; Z. Zhou; L. Deng; H. Guo; M. Xie; F. Qi, Angew. Chem. Int. Ed. 49 (2010) 3169-3172
12. A. J. Eskola; O. Welz; J. Zador; I. O. Antonov; L. Sheps; J. D. Savee; D. L. Osborn; C. A. Taatjes, Proceedings of the Combustion Institute 35 (2015) 291-298 10.1016/j.proci.2014.05.011.
13. D. L. Osborn; P. Zou; H. Johnsen; C. C. Hayden; C. A. Taatjes; V. D. Knyazev; S. W. North; D. S. Peterka; M. Ahmed; S. R. Leone, Rev. Sci. Instrum. 79 (2008) 104103 DOI: 10.1063/1.3000004.
14. A. J. Eskola; O. Welz; J. D. Savee; D. L. Osborn; C. A. Taatjes, J. Phys. Chem. A 117 (47) (2013) 12216-12235 10.1021/jp408467g.
15. A. Jalan; I. M. Alecu; R. Meana-Paneda; J. Aguilera-Iparraguirre; K. R. Yang; S. S. Merchant; D. G. Truhlar; W. H. Green, Journal of the American Chemical Society 135 (30) (2013) 11100-14 10.1021/ja4034439.